Clinical application of intensity and energy modulated radiotherapy with photon and electron beams

Xiangkui Mu

Department of Radiation Sciences, Oncology
Umeå University
2005

© Mu Xiangkui
Department of Radiation Sciences, Oncology
Umeå University 2005

Printed by Print & Media, Umeå University

January 2005:2000657

ISBN 91-7305-793-2

ISSN 0346-6612

To my wife, daughter and my parents

致知在格物

《孔子·大学》

路漫漫其修远兮，吾将上下而求索

《屈原·离骚》

Table of Contents

Abstract	2
Abstract in Chinese	3
List of papers	4
Abbreviations	5
Introduction	6
Aims of the study	11
The influence of prolonged fraction time on the radiation effect (I)	12
Properties of electron beams (II, III)	18
The added value of electrons to IMXT (II)	19
Intensity and energy modulated electrons (III)	22
Side-effects in paediatric therapy and further improvement of the dose conformity with protons (IV)	28
Conclusions	33
Acknowledgements	36
References	38

Abstract

In modern, advanced radiotherapy (e.g. intensity modulated photon radiotherapy, IMXT) the delivery time for each fraction becomes prolonged to 10-20 minutes compared with the conventional, commonly 2-5 minutes. The biological effect of this prolongation is not fully known.

The large number of beam directions in IMXT commonly leads to a large integral dose in the patient. Electrons would reduce the integral dose but are not suitable for treating deep-seated tumour, due to their limited penetration in tissues. By combining electron and photon beams, the dose distributions may be improved compared with either used alone. One obstacle for using electron beams in clinical routine is that there is no available treatment planning systems that optimise electron beam treatments in a similar way as for IMXT. Protons have an even more pronounced dose fall-off, larger penetration depth and less penumbra widening than electrons and are therefore more suitable for advanced radiotherapy. However, proton facilities optimised for advanced radiotherapy are not commonly available. In some instances electron beams may be an acceptable surrogate.

The first part of this study is an experimental *in vitro* study where the situation in a tumour during fractionated radiotherapy is simulated. The effect of the prolonged fraction time is compared with the predictions by radiobiological models. The second part is a treatment planning study to analyse the mixing of electron and photon beams for at complex target volume in comparison with IMXT. In the next step a research version of an electron beam optimiser was used for the improvement of treatment plans. The aim was to develop a method for translating crude energy and intensity matrices for optimised electrons into a deliverable treatment plan without destroying the dose distribution. In the final part, different methods of treating the spinal canal in medulloblastoma were explored in a treatment planning study that was evaluated with biological models for estimating risks for late radiation effects.

The effect on cell survival of prolonging fraction time at conventional doses/fraction is significant in an *in vitro* system. This effect is underestimated by biological models. Prolonging the fraction time will spare tissues with a fast DNA repair. Thus, there is a risk for sparing tumours. The mixed electron and photon beam technique has the potential to treat deep-seated tumours. Compared with IMXT the number of beams can be reduced and as a consequence, the time for each fraction could be kept shorter. The integral dose in the patient will also be lower. The mixed beam technique could potentially be further improved if automatic optimisation for electrons was available. The results suggest that optimisation and segmentation can be automated, and a deliverable treatment plan can be obtained with simple procedures without destroying the quality of the dose distribution. The integral dose in patients may lead to late radiation side-effects. In childhood cancers the risk for development of radiation induced cancers is a reality and the integral dose outside the target volume should be minimised. Based on models for cancer induction, protons show the lowest risk while electrons have some benefit compared with different photon techniques. All methods are able to similarly well treat the target volume.

Keywords: Radiotherapy, intensity modulated radiotherapy, IMXT, IMET, IMPT, proton beams, electron beams, treatment planning, cancer induction, side-effects, fraction time.

论文摘要：

先进的放射治疗，如调强放射治疗（IMXT），其单次照射时间可以被延长到10到20分钟（传统放射治疗的单次照射时间约2到5分钟）。目前，单次照射时间延长引起的放射生物学效应的改变并不清楚。

IMXT使用比传统放射治疗更多的射束，增加了病人的累积受照剂量。因为电子线在物质内的穿透深度是有限的，使用电子线可以减小病人的累积受照剂量，但电子线不适合治疗深部肿瘤。电子线和X线混合照射可能提高电子线或X线的剂量分布。目前，阻碍电子束调强技术在应用于临床的主要原因可能是治疗计划系统不具有电子束调强的功能。与电子线相比，质子治疗有更快的剂量衰减，更深的穿透深度，更窄的半影，因而更适合先进的放射治疗技术。但质子治疗设备昂贵、复杂，目前不能广泛的在放射治疗中心配备。因此，在目前的某些情况下，电子线可作为质子射束的一种替代选择。

该研究的第一部分研究了分次照射时间延长对放射生物学效应的影响。该研究使用离体细胞模拟肿瘤接受放射治疗的情形（相同的剂量，不同的照射时间），并与放射生物学模型计算的预测值进行比较；第二部分研究了电子线和X线混合照射在治疗深部肿瘤时的剂量分布，并与IMXT的进行了比较。第三部分研究了计算机化电子束调强程序，目的是找出将优化后的电子束能量和强度的矩阵转换成可以治疗的治疗计划。最后，研究评价了不同放射治疗技术（传统光子、电子线技术，IMXT，电子束调强技术，质子调强技术）在髓母细胞瘤脊髓照射中的应用。使用生物学模型对晚期放射反应，特别是放射线诱发的第二原发肿瘤的几率进行了评估。

在传统分次剂量范围内，在离体细胞系中，分次照射时间延长产生的放射生物学方面的影响是显著的。而且，放射生物学模型低估了这个影响。照射时间延长将保护快DNA修复组织。因此，存在保护肿瘤的危险。混合电子线和X线照射技术可以用来治疗深部肿瘤。与IMXT相比，混合照射可以减少射束数目，因而缩短照射时间，并可以减少病人的累积照射剂量。如果使用自动的电子束调强程序，混合线照射的剂量分布可以得到进一步提高。第三部分的研究结果显示，自动的电子束调强治疗可以实现，而且可以通过简单的步骤将电子线能量和强度的矩阵转换成可以治疗的治疗计划。该研究的第四部分结果表明，肿瘤区域外的累积剂量可能引起晚期放射反应，特别是在儿童肿瘤病人中，放射线诱发的第二原发肿瘤是一个现实问题，因此当代的放射治疗技术应该尽量的降低肿瘤区域外的累积剂量。与传统照射方式相比，质子诱发第二原发肿瘤的几率最低，其次是电子束调强技术。

关键词：放射治疗，调强放射治疗，IMXT，IMET，IMPT，质子束，电子束，治疗计划，诱发肿瘤，副反应，分次照射时间。

List of papers

This thesis is based on the following papers, which will be referred to in the text by their roman numerals:

I. Xiangkui Mu, Per-Olov Löfroth, Mikael Karlsson and Björn Zackrisson. The effect of fraction time in intensity modulated radiotherapy: theoretical and experimental evaluation of an optimisation problem. Radiother Oncol. 2003; 68(2):181-7.

II. Xiangkui Mu, Lennart Olofsson, Mikael Karlsson, Rickard Sjögren and Björn Zackrisson. Can photon IMRT be improved by combination with mixed electron and photon techniques?.Acta Oncol. 2004; 43(8): 727-35.

III. Xiangkui Mu, Lennart Olofsson, Simeon Nill, Uwe Oelfke, Michael Karlsson, Björn Zackrisson. Heart sparing in chest wall irradiation: computer-aided electron optimisation. (Submitted)

IV. Xiangkui Mu, Thomas Björk-Eriksson, Simeon Nill, Uwe Oelfke, Karl-Axel Johansson, Giovanna Gagliardi, Lennart Johansson, Mikael Karlsson, Björn Zackrisson. Does electron and proton therapy reduce the risk for late-effects after spinal irradiation for childhood medulloblastoma? – A comparative treatment planning study. (Submitted)

The original papers have been reproduced with permission from the publishers.

Abbreviations

3-D CRT	Three dimensional conformal radiotherapy
CT	Computer tomography
CTV	Clinical target volume
DVH	Dose volume histogram
ICRP	International Commission on Radiological Protection
ICRU	International Commission on Radiation Units and Measurements
IMXT	Intensity modulated radiotherapy with photons
IMET	Intensity and energy modulated radiotherapy with electrons
IMPT	Intensity and energy modulated radiotherapy with protons
IMRT	Intensity modulated radiotherapy
LKB model	Lyman-Kutcher-Burman model
MLC	Multi-leaf collimator
MB	Mixed electron and photon beam plan
NTCP	Normal tissue complication probability
OARs	Organs at risk
PTV	Planning target volume
RBE	Relative biological effectiveness
RS model	relative seriality model
SLC	Radiation induced secondary lethal cancer
SOBP	Spread out Bragg Peak
TCP	Tumour control probability

Introduction

Since the birth of radiotherapy in the last years of the 19th century the therapy techniques have continuously been improved and refined in parallel to technical improvements and increased radiobiological knowledge. The innovations during the last decades are to a major extent based on the development in medical imaging and computer sciences. Today, imaging helps the radiation oncologists to delineate the tumour target more precisely than ever before. Computers are now involved in every step of the process of radiotherapy.

The ideal radiotherapy would be to deliver a radical radiation dose to tumour cells, and no dose to normal tissues (Fig. 1). Ionising radiation causes damages in normal tissues that can be classified as deterministic (mainly due to cell killing) and stochastic (due to mutation) effects (1, 2). Deterministic effects, such as serious malfunction or necrosis, become evident when the irradiation in tissue reaches a threshold dose (usually >1-2 Gy). Above the threshold dose the severity of effects increase with the increase of dose. For stochastic effects there is no threshold dose, and the severity of effects is independent of the dose.

In radiotherapy, normal tissues are virtually always irradiated with a certain doses, the magnitude depends on the technique used (Fig. 1). This is especially the case when the organs at risk (OARs) are situated close to a deep-seated tumour target. The improvement of techniques for conformity of the dose distribution to the tumour volume and for decreasing the dose in normal tissues is a major theme in radiotherapy research.

Protons have physical properties that make them possible to use for producing more conformal dose distributions than with conventional x-rays and/or electrons in most cases (Fig. 1). As compared with photons, almost zero doses are delivered to the volume downstream the target and lower doses to the volume in front of the target. The dose distribution of protons can be further improved by intensity and energy modulation techniques (IMPT) (3, 4). Due to the technical complexity and the cost of

proton facilities, hospital based protons are today only available in a few academic hospitals in the world.

Conventional external radiotherapy uses photon and/or electron radiation. Megavoltage photons are used for deep-seated tumours. A single photon beam will usually deliver more absorbed dose to the normal tissue in front of the tumour. Therefore, multiple beams incident from different angles are employed in clinical practice. Electrons are mainly used for more superficial targets. Electrons have a fast dose fall-off at depth that makes them suitable for treatments where critical structures are localised behind the tumour (Fig. 1). Possibly the lack of equipment that is optimised for effective electron delivery and planning explains the very limited use of advanced electron techniques.

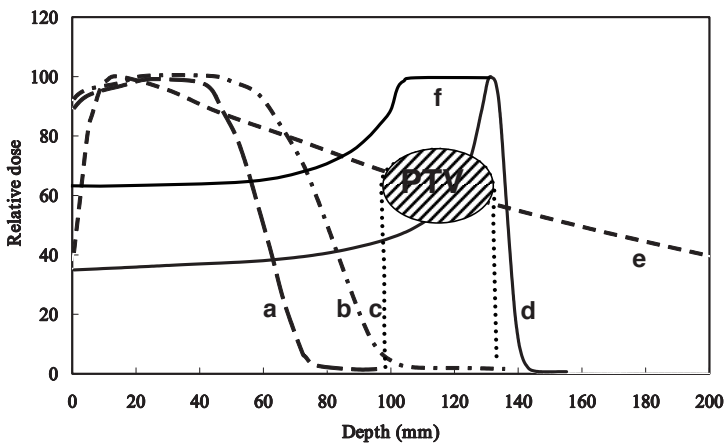

Figure 1. Depth dose distribution for a treatment with single beam of 15 MeV electron (a), 20 MeV electron (b), ideal dose distribution (c), 6 MV photon (e), and spread out Bragg Peak (SOBP) of 150 MeV proton beam (f). PTV is showing the tumour target, and (d) shows the depth dose of mono-energetic protons of 150 MeV

Since more than a decade, three-dimensional conformal radiotherapy (3-D CRT) has become a focus of radiotherapy development. The technique requires computer tomography (CT) for obtaining information of the tumour volume and OARs and computerised treatment planning for virtually displaying dose distribution. Typically, a 3-D CRT photon plan is produced by applying multiple beams from several directions,

coinciding in the centre of the planning target volume (PTV). The beams are shaped to match the projection of the PTV with multi-leaf collimators (MLC) or blocks. The intensity within each beam is typically uniform or may be modified by simple devices as wedges. The dose distribution of 3-D CRT is often closely conformed to the shape of a PTV with convex or plane surfaces, and the dose to the surrounding normal tissues can be kept low (5).

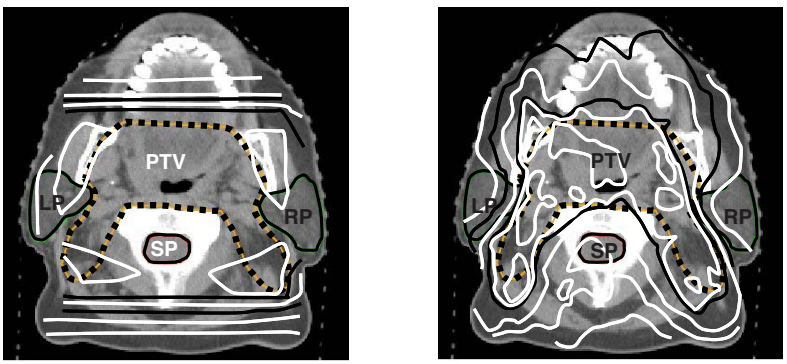

Figure 2. The dose distribution for (a) 2 lateral opposed photon beams and (b) 7 evenly distributed intensity modulated photon beams. Isodoses for 10%, 30%, 50%, 70%, 90%, and 100% are indicated. The isodose lines for 50% and 90% are in solid black lines, others are in white. LP and RP are left and right parotid glands respectively. SP is the spinal canal.

In cases where the PTV has one or more concave surfaces, especially when OARs are partly surrounded by the PTV, 3-D CRT may not able to deliver a radical dose to the tumour without exceeding the tolerance dose of OARs. One solution to this problem is intensity modulated x-ray radiotherapy (IMXT) (6, 7). (Fig. 2)

The definition of IMXT has been given by the IMRT Collaborative Working group: “An advanced form of 3D-CRT that uses non-uniform radiation beam intensities, incident on the patient, that have been determined using various computer-based optimization techniques” (8). By IMXT, dose distributions that fulfil the clinical requirements better than 3-D CRT can be obtained for several complex target shapes (9-11).

One clinical motive for developing 3-D CRT and IMXT was the hypothesis that a higher radiation dose to the tumour target should give a higher probability for tumour control. This would be possible to achieve without increasing the risk for side-effects. No clinical evidence in the form of prospective randomised clinical studies has yet been presented concerning the tumour control of IMXT vs. e.g. 3-D CRT (8, 12, 13). Until such data are available, potential advantages as well as disadvantages of IMXT must be explored in other ways. Alternatively, the therapeutic gain could be utilised for decreasing the risk for serious side-effects and maintaining the tumour control probability. Clinical results that support this theory have been reported for some tumour sites (14-16). Till now, the dominating use of IMXT has been for head and neck cancer (17-19), prostate cancer (11, 20), breast cancer (21, 22), paediatric cancer (23), and other body sites (24).

IMXT seems to offer several improvements to radiotherapy compared with previous techniques. However, as with all new developments there are some potential risks and/or concerns that need to be addressed. Some consequences of the IMXT technique are; the prolonged dose delivery time; the large integral dose in the surrounding normal tissues; inhomogeneous dose in the target volume (25); the complexity of technique and the demand of human resources and facilities (26). Some of these potential problems have been addressed in this thesis.

The first part of the project concerned the prolonged fraction time (from the beginning of the first beam to the end of the last) that frequently is a consequence of IMXT. We carried out an in vitro experimental study to investigate the effect of the changes in fraction time. Different biological models were used for predicting the effect of prolonged fraction time (Paper I). One way of reducing the fraction time in IMXT could be to reduce the complexity of the beam delivery. One possible way of accomplishing this could be to mix conventional photon-IMXT with electrons (Paper II). As opposed to photons, electrons have an energy dependent dose fall-off at depth. This property might facilitate the shaping of conformal dose distributions in complex target volumes. Furthermore, the integral dose might be reduced since the electrons would contribute to less radiation dose downstream the target volume than photons

(Paper II, III). Treatment planning with computerised optimiser for electron is essential for energy and intensity modulated electron therapy (IMET). Today, only few planning system are capable of optimising electron, but not producing a deliverable IMET plan due to the large variations in both energy and intensity in each beam. In this thesis a method (for the same purpose as the "sequencer" in IMXT planning system) to transform the results from an electron beam energy-fluence optimiser into a deliverable treatment plan was developed (Paper III).

Even though the high dose in surrounding normal tissues is decreased, IMXT frequently delivers a low dose to a larger volume of tissues outside the tumour target than many traditional external radiotherapy techniques do. The risk for deterministic effects after very low-dose irradiation in normal tissues is yet unknown. Because most data on this unwanted effect are collected from treatments delivered with conventional techniques thus, usually a higher dose is delivered to surrounding normal tissues. However, some evidence shows that even low total doses (5Gy – 12.5 Gy) of radiation may result in late side-effects such as excessive fibrosis or scar-tissue formation, probably due to cytokine activation (27). However, these radiation doses are so low that it may take many years for the effects to appear. A low dose hypersensitivity has been observed for doses <1 Gy (28). The clinical relevance of this phenomenon is not yet fully understood but it might contribute to late side-effects. The risk for stochastic effects associated with low dose irradiation, such as cancer induction, may cause more concerns, particularly in a paediatric group. The relevant, induced mutation occurs in cells that survive the irradiation. Thus, a low dose (<1-2 Gy) is sufficient to cause these effects (1). Children are probably more sensitive to radiation due to more active cell proliferation. In Paper IV different treatment strategies with photons, electrons and protons for spinal canal treatment in medulloblastoma in children are analysed and discussed with respect to possible long term toxicity and radiation induced secondary lethal cancer (SLC).

Aims of the study

The developments of new radiation techniques in recent years have improved the possibility to tailor the dose distributions to the shapes of the target volumes. As a consequence of the new advanced techniques, the fraction time risks to be prolonged. Furthermore, the volume of normal tissues which are irradiated to low doses will be increased. These potential problems as well as some possible solutions to them have been explored according to the following specific aims

- To investigate how prolonged fraction time changes the biological effectiveness of radiotherapy (I).
- To investigate if the combination of electrons and photons can improve the dose distribution of photon IMRT, and the efficiency of dose delivery (II).
- To investigate the possibility of transforming an electron energy and intensity matrix from an automatic optimisation procedure into a clinically deliverable treatment plan (III).
- To investigate the physical dose distributions created for different treatment techniques in the spinal canal irradiation in children with medulloblastoma and explore their possible importance for late side-effects, particularly for SLC (IV).

The influence of prolonged fraction time on the radiation effect (I)

The time for one fraction from start of treatment on the first field to the end of the last will often increase proportionally to the complexity of treatment technique. In the commonly used IMXT delivery techniques, the treatment time may be up to 15 minutes for a static segmental IMXT plan with 50-60 MLC segments (29, 30). The delivery time is about 10-12 minutes for dynamic IMXT with 5 or 6 beams, (10). For tomotherapy, the delivery time is directly proportional to the length and volume of the lesion. A single rotational arc takes approximately 5-10 minutes and with a typical plan of 3-4 couch increments, total delivery times are between 15-30 minutes (30).

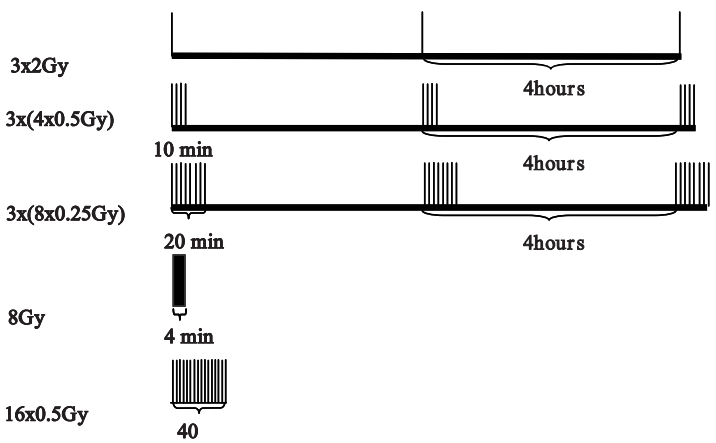

Figure. 3. Illustration of the delivery of radiation dose, fraction sizes, and divisions of fractions into sub-fractions in the experiments of this study.

The biological effects of increased fraction time can be predicted by the use of different biological response models. However, the predictions might differ between models. This makes the testing of models under these circumstances important. Consequently, in vitro experiments where some basic variables can be controlled will make the interpretation simpler and act as a first step in the process of testing the model. Therefore, evaluation of the predictive ability of radiobiological models by experiments is needed.

In Paper I, we carried out an in vitro experimental study to investigate the effect of changes in fraction delivery time. A dose of 2 Gy was delivered to cultured hamster fibroblasts (V79-379-A) cells in 1, 10, and 20 minutes. Each fraction was divided into sub-fractions to simulate the delivery of IMXT. In order to evaluate the models for higher doses per fraction than 2 Gy, and compare with previous experimental data (31), a dose of 8 Gy was delivered to V79 cells in 4 minutes and 40 minutes (Fig. 3).

The basic LQ-model was developed to simulate the biological effect of single dose irradiations given to different dose levels at intervals large enough for sub-lethal damages to recover between irradiations (32).

$$S = \exp(-\alpha \cdot D - \beta \cdot D^2) \qquad \text{(Eq. 1)}$$

where, S is the surviving fraction of V-79 cells after irradiation. α and β are constant parameters characterising the biological system and D is the total absorbed dose.

In the study of fractionated regimes, a common modification of LQ-model by superposition of single fraction survival has been used. The surviving fraction for different regimes can thus be described by the following equation (32):

$$S = \exp(-n \cdot \alpha \cdot d - n \cdot \beta \cdot d^2) \qquad \text{(Eq. 2)}$$

To describe the biological effect of treatment given with low dose rate or with many sub-fractions in each fraction, a factor G is multiply to the quadratic term in the fractionated LQ-model to correct the effects of incomplete repair of sub-lethal damages. Then, the surviving cell fraction can thus be described as:

$$S = \exp(-n \cdot \alpha \cdot d - G \cdot n \cdot \beta \cdot d^2) \qquad \text{(Eq. 3)}$$

Where, G is a correction for incomplete repair.

Already Lea and Catheside (33) presented ideas with a dose rate correction function based on data from continuous irradiation with low or moderate dose rate. In mathematical form, the G in Eq.3 can thus be represented by G_T in Eq. 4 (34, 35).

$$G_T = \frac{2 \cdot \tau}{T_\delta} \cdot \left[1 - \frac{\tau}{T_\delta} \cdot (1 - x) \right] \quad \text{(Eq. 4)}$$

Where, T_δ is the dose delivery time of one fraction, τ is the recovery time of sub-lethal damages, and x is representing the exponential decay of sub-lethal damage.

$$x = \exp\left(-\frac{T_\delta}{\tau} \right) \quad \text{(Eq. 4b)}$$

$$\tau = \frac{T_{1/2}}{\ln(2)} \quad \text{(Eq. 4c)}$$

$T_{1/2}$ is the half time of sub-lethal repair.

In the incomplete repair (IR) model (35), gave an expression, which assumes no recovery during actual irradiation but rather during the time between fractions, i.e., applies to acute fractions. Here we will use the expression mainly for sub-fractions within one 2 or 8 Gy fraction, taking G in Eq. 3 equal to $G_{\delta T}$, with

$$G_{\delta T} = \frac{2}{(n')^2} \left[\frac{\theta}{1-\theta} \right] \cdot \left[n' - \frac{1-\theta^{n'}}{1-\theta} \right] + \frac{1}{n'} \quad \text{(Eq. 5a)}$$

Where θ is representing the exponential of sub-lethal damage according to

$$\theta = \exp\left(-\frac{\delta \cdot T}{\tau} \right) \quad \text{(Eq. 5b)}$$

n' is the number of sub-fractions in one fraction (e.g., *n'* = 1,4,8,or 16), and δT is the time interval between different sub-fractions within one fraction (Table 1). The short irradiation duration for any one sub-fraction is regarded as incorporated appropriately into δT.

Parameters of the basic cell survival curves (α, β) and repair kinetics (τ) were established in this cell line (see Paper I).

α =0.16 Gy^{-1} (S.D. 0.04)

β=0.016 Gy^{-2} (S.D. 0.003)

$T_{1/2}$=0.4 h and thus τ =0.58 h

The experiments showed that the prolongation of the dose delivery time is sparing tissues with a fast DNA repair. In the comparison of results from the different sub-fractionations experiments, S_{1min} were used as reference and the results are presented as ratios of surviving fractions after prolonged and acute exposure (Fig. 4). In the experiment where 2 Gy fractions were delivered either in one fraction in one minute or in a number of sub-fractions in 10 or 20 minutes, a statistically significant difference between the groups was found ($p<0.001$). For 8 Gy fractions, there was a statistically significant difference between the 40 minutes irradiation and 4 minutes irradiation ($p<0.001$). In this case, S_{4min} was used as a reference and the results are presented as ratios of surviving fractions. From survival fraction curves (Fig. 4 in Paper I), the relative biological effectiveness (RBE) was calculated. For 2Gy fraction size, $RBE_{10min/1min}$ was 1.15, $RBE_{20min/1min}$ was 1.19. For a fraction size of 8Gy, $RBE_{40min/4min}$ was 1.12, which is similar to experiments on human skin for large fraction sizes (31).

The results also show that the biological models underestimate the effect of prolonged fraction times at conventional dose/fraction. For 2 Gy fractionations the models greatly underestimated the effect seen in the experiments (Table 1, Fig. 4). However, for 8 Gy fractions, a good agreement was found between experimental results and those predicted by the models (Table 1, Fig. 4). The same irradiation regimes were analysed with models for both sub-fractionated and different dose rate routines. It is worth noting that both types of models give very similar results.

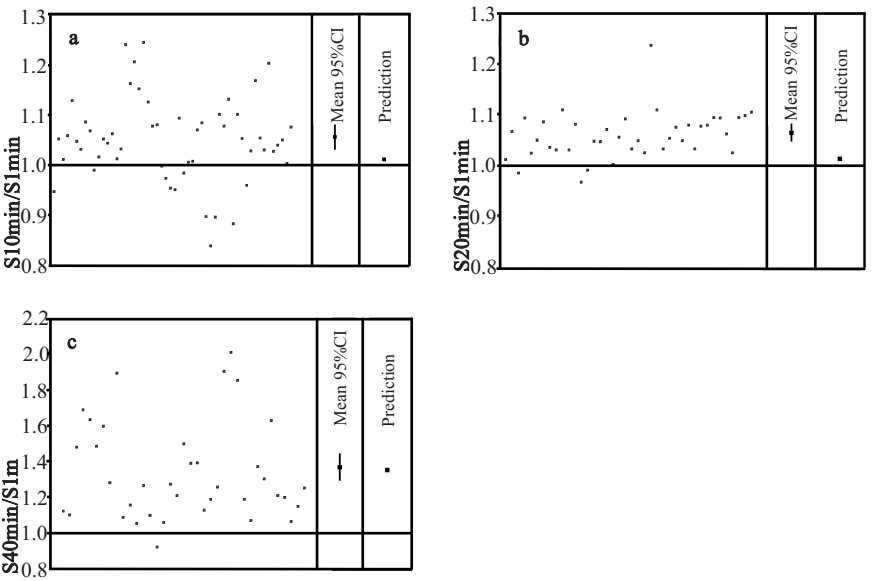

Figure 4. Plot of the ratios of surviving fraction of different sub-fractionation experiments to acute exposure, ratio mean and 95% confidence intervals, and predicted values according to Eq. (4), for a) $S_{(10min)}/S_{(1min)}$ for 2 Gy fractions, b) $S_{(20min)}/S_{(1min)}$ for 2Gy fractions, and c)$S_{(40min)}/S_{(4min)}$ for an 8Gy fraction.

Table 1. Comparison between experimental survival data and those predicted by the different models. The models have been applied both with the number of sub-fractions as parameter and with the total time used as varying parameter. *n'*, d, T_δ and δT are parameters used in the models. The ratio of surviving cells compared with an acute irradiation is given by S-ratios, $S_{T\delta}$ (33), $S_{\delta T}$ (35), as in the equations 4 and 5 respectively.

Treatment	S-ratio Experiment	*n'*	d* Gy	T_δ min	δT min	$S_{T\delta(ref)}$ ratio	$S_{\delta T}$(ref) ratio
2Gy-S_{4f}/S_{1f}	1.054 (±0.025)	4	0.5	------	3.33	-------	1.009
2Gy-S_{8f}/S_{1f}	1.063 (±0.017)	8	0.25	------	2.86	-------	1.014
2Gy-S_{16f}/S_{1f}	-------	16	0.125	------	2.67	-------	1.022
8Gy-S_{16f}/S_{1f}	1.370 (±0.070)	16	0.5	------	2.67		1.37
2Gy-S_{10min}/S_{1min}	1.054 (±0.025)	1	2	10	------	1.007	-------
2Gy-S_{20min}/S_{1min}	1.063 (±0.017)	1	2	20	------	1.012	-------
2Gy-S_{40min}/S_{1min}	-------	1	2	40	------	1.021	-------
8Gy-S_{40min}/S_{4min}	1.37 (±0.070)	1	8	40	------	1.35	-------

In sub-fractionated routines, d* is dose per sub-fraction; in difference dose rate routines d* is dose per fraction.

From the results, we can draw the following conclusion: For a tissue with S_{2Gy} of 0.67 and $T_{1/2}$ of 0.4 h, as in Paper I, a prolongation of treatment time for each fraction from 5 to 20 minutes would lead to approximately 1 log less cell kill after 32 fractions. In the present example this would mean that for the prolongation of fraction time from 1 to 20 minutes, either fraction size or number of fraction need to be increased about 15 - 19% to reach the same cell kill. For example, if the prescription dose to the tumour was 2 Gy in 1 minute for 32 fraction, 10 minutes fraction time would demand 37 fractions, and 20 minutes 39 fractions; Otherwise, 15 - 19% increased fraction size is needed to compensate for the prolonged fraction time. This correction would then only be valid for one specific tissue, e.g. tissues with longer $T_{1/2}$ would be less spared by the long fraction times and thus, be subjected to more severe radiation effect.

Properties of electron beams (II, III)

Electrons are commonly used for treating superficial target, such as chest wall, lymph node metastases, and in head and neck cancers. The limited depth range of electrons minimises the doses to the normal structures downstream the tumour. However, the penumbra of electron beams widens with increasing depth in the patient. Thus, the effective treatment field is getting smaller (Fig. 8). When treating deep-seated tumour, the fast dose fall-off becomes a disadvantage (Paper II).

Several research groups have investigated the possibility of improving the properties of electron beams (36, 37). For example, dose distribution of electron beams have been improved by combining them with photon beams. The addition of a low-weight, wedged, photon beam perpendicular to the distal part of an electron beam increases the effective treatment depth of the electron beam (36). Adding a narrow photon beam to the electron beam edges beam reduces the electron beam penumbra and enlarges the effective field size (37, 38). Matching different electron energies to obtain a desired dose gradient (39-41). Mixed different electron energies to obtain the depth range corresponding to the median energy or increase dose in beam build up region of high energy electron (42). Some reports focused on intensity modulated electron beams with 3-D bolus (43) or electron MLC (44, 45). In Paper II, we applied most techniques described above to create a complex dose distribution for a deep-seated tumour target.

The added value of electrons to IMXT (II)

Cancer of the head-and-neck is a common indication for IMXT, because of the many OARs that exist in the region. Irradiation of these structures may lead to serious late complications, such as xerostomia. IMXT may improve this side-effect, hence improving the quality of life (15, 46-48). However, the integral dose to the surrounding normal tissues may increase with IMXT. This may introduce risks particularly for the long-term survivors who may be at risk of secondary, radiation induced, cancers (49). Other unwanted side-effects might be caused by low-dose hypersensitivity (28), although the clinical implications of this phenomenon is still not fully understood.

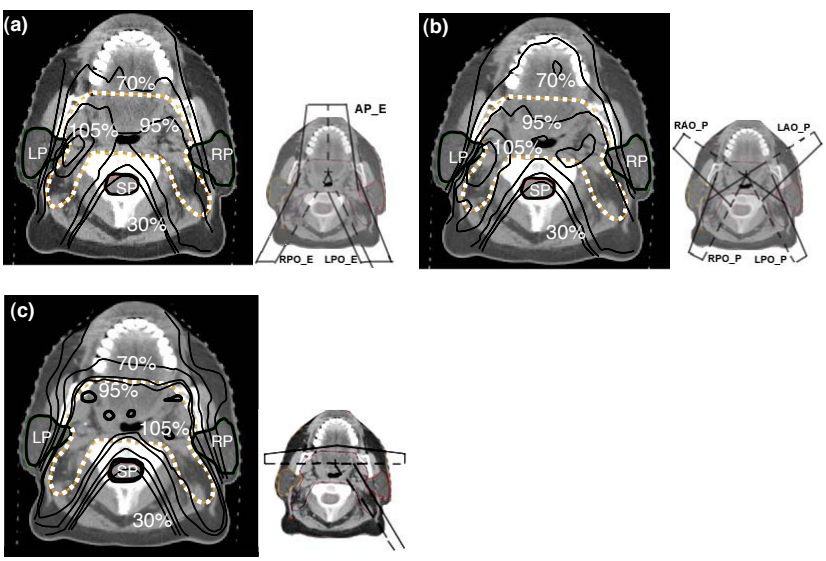

Figure 5. The procedures of mixed beam forward planning. Three main electron-beam directions are from anterior and oblique posterior, which avoid direct irradiation of the OARs. Three photon beams were added in the same beam direction as the three main electron beams (Fig. 5a). Additionally, two anterior oblique photon beams were added, in order to improve the dose in the central region of target, and to reduce the skin dose (Fig. 5b). Two laterally opposed, low-weight, narrow photon beams covered the anterior part of target. Six to nine small photon beams and electron beams from the directions described above were added to improve the dose homogeneity within the target (Fig. 5c).

The added value of electrons to IMXT from aspects of the reduction of integral dose in normal tissues and the improvement of efficiency of dose delivery was investigated in

Paper II. Treatment plans were made for five simulated head and neck cancer cases. Mixed electron and photon beam plans (MB) were constructed using a manual iterative procedure with TMS 6.0 (Nucletron B.V., The Netherlands). Photon-IMXT plans were optimised automatically with OTP1.2 (Nucletron B.V., Netherlands.). Both electron and photon beams were collimated by a computer controlled MLC. The goal of both treatments is to deliver a mean dose of 70 Gy to the tumour target with a dose variation of not more than ± 10%; and constraints OARs were set to a mean dose of less than 26 Gy to both parotids (15), maximum dose of 50 Gy to spinal cord and of 60 Gy to brainstem.

The approach with opposite bilateral electrons was not used for this study, since the thickness of the patients often precludes the use of such techniques with electrons of conventional energies (<25 MeV). In addition, the absorbed dose in the parotid region exceeds the dose-volume constraint for the parotids (Fig. 1 in Paper II). Therefore, alternative technique was used (Fig. 5).

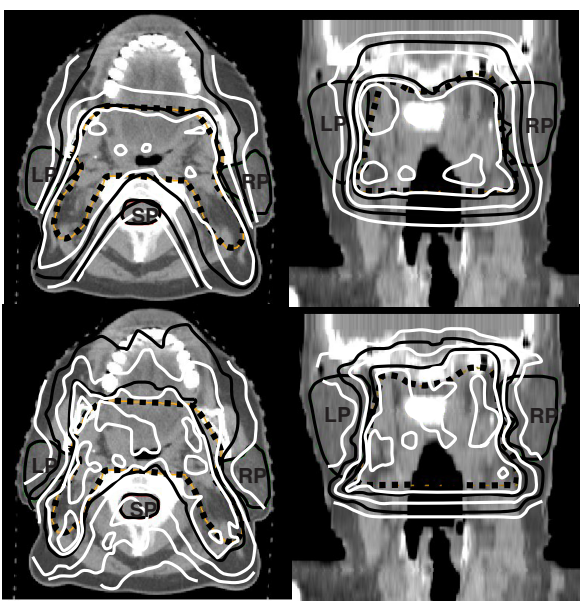

Figure 6. Dose distribution of patient no. 4 for both the mixed electron and photon beam plan and the photon IMRT plan with isodose lines 30%, 50%, 70%, 90%, 95% and 105%. Isodose lines of 50% and 90% are in black. LP and RP are left parotid and right parotid. SP is spinal cord. PTV is shown with black dotted ine.

Results showing that MB technique deliver less integral dose to the surrounding normal tissues ($p < 0.05$), and similar target coverage as IMXT technique dose (Figs 6, 7 and Table 1 in Paper II). For the parotid glands the results are similar with both techniques. However, the dose volume histograms (DVH) of spinal cord and brain stem indicate that there is a margin for further optimisation in the MB plans. The same beam angles were used both in MB and IMXT techniques, but fewer segments in MB plans (15-20 segments) than in IMXT plans (54-62 segments)

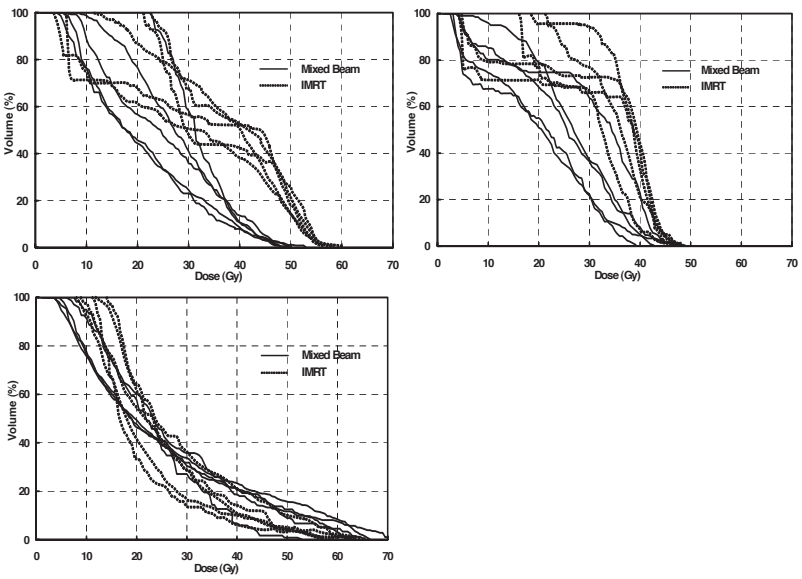

Figure. 7. DVHs for left parotid, spinal cord and brain stem for both mixed electron and photon plans (solid line) and photon IMRT plans (dotted lines).

Intensity and energy modulated electrons (III)

There are at least two main reasons for the limited use of IMET in clinical radiotherapy. One is that most commercial accelerators are not equipped and optimised for multi-leaf collimated electrons. This problem can be solved with quite moderate modifications of conventional linear accelerators (50-53). So far, it is only the racetrack microtron (MM50, IBA, Belgium) that fulfils these requirements. Another problem is that the treatment planning process with range optimisation as a major component is often laborious if it is performed with conventional forward planning. Commercial systems are usually not equipped with such algorithms. However, an algorithm-based energy/range-selection method for electron optimisation has been presented (42).The algorithm uses the large field electron range (energy/range optimiser) to select electron energies corresponding to the distal edge of the PTV. Three energy layers are weighted by an intensity optimiser to adjust the energy selection and distribution. This energy-selection method handles both the energy and the intensity-optimisation.

In Paper III, we analysed the techniques for compensating the electron scatter in the beam edges in IMET (Fig. 8) and defined a method to transform electron energy and intensity matrices into a deliverable treatment plan.

The treatment planning simulation was done on a breast cancer patient who had a left sided cancer after mastectomy. The thoracic wall and the ipsilateral internal mammary nodes were defined as CTV. The left lung and the heart were outlined as the OARs. A dose of 50 Gy was delivered as the mean to the PTV. The dose homogeneity within the PTV was planned to be ± 10%.

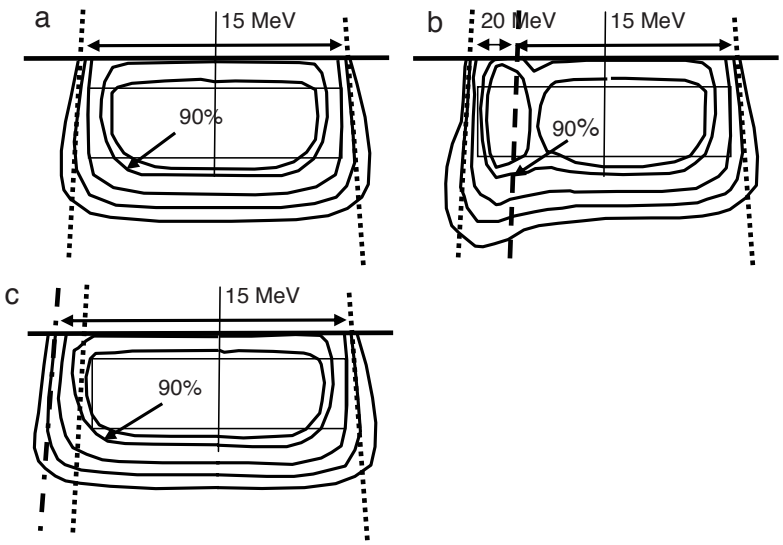

Figure 8. Illustration of the principle for beam edge compensation. A 10 cm wide, rectangular target (thin line) treated with 15-MeV electrons is shown. The 30%, 50%, 70%, 90% and 95%, isodose lines are shown. (a) shows an under dosage to the lateral border of PTV due to the lack of inward scattered electrons. In (b) the left lateral part of the beam is replaced by a narrow, equally weighted, 20-MeV electron beam. This compensates the lack of inward scattered electrons, but the absorbed dose downstream from the target is increased. (c) shows the effect of an extra beam margin to the PTV. This compensates the lack of inward scattered electrons close to the PTV and avoids the absorbed dose downstream from the target but results in an increased dose laterally.

The IMET plans were produced in a modified research version of the KonRad program (DKFZ-Heidelberg, Department of Medical Physics, Germany). The IMET plan for energy compensation approach was obtained with a 3-step procedure. The primary energy selection was performed according to the method described by Olofsson et al (42). The energy modulation was realised by adding two additional energy layers of -2.5 MeV and + 5 MeV. Finally, the intensity optimiser determines the intensity for each energy in the beam matrices (42); The IMET plan for wide margin approach was obtained with similar procedures as energy compensation approach, the differences were that the energy matrices have an extra margin of 1 cm compare with those in energy compensation plan and the energy of two additional energy layers were -2.5 MeV and + 2.5 MeV (Fig. 9a, see Paper III). A four-segment electron plan was constructed following the local clinic routine (40) with an isocentric

technique (see Paper III). The plan was transferred to the optimiser for dose recalculation. The results were used as the baseline for further comparisons with IMET plans.

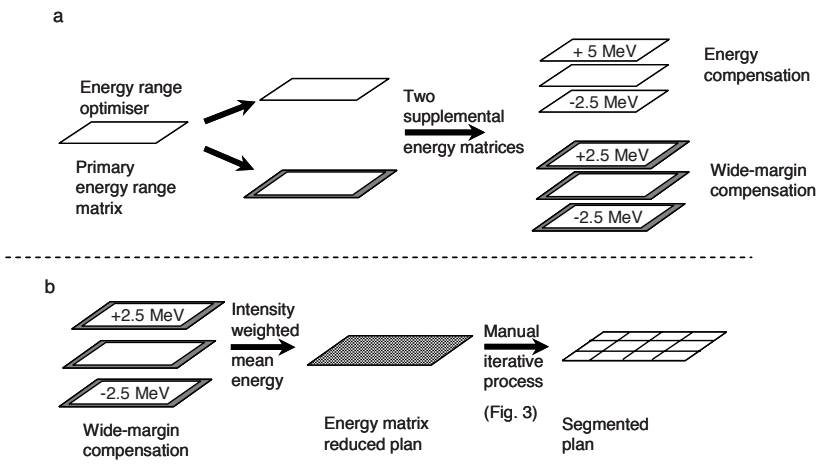

Figure 9. (a) shows the procedure for "energy compensation" and the "wide-margin compensation" after the primary energy range optimisation. (b) shows schematically the process of segmentation. The iterative manual procedure for the final segmented treatment plan is shown in detail in Fig. 10.

The optimisation creates a more conformal dose distribution than the forward plan. However, the dose can not be delivered directly with the information of the energy and intensity matrices given by the optimiser. A deliverable treatment plan has to be produced without significant changes of the dose distribution. Based on the wide-margin compensation plan, a deliverable plan was created in a three-step procedure (Fig. 9b, see Paper III).The iterative manual procedure for the final segmented treatment plan is shown in detail in Fig. 10.

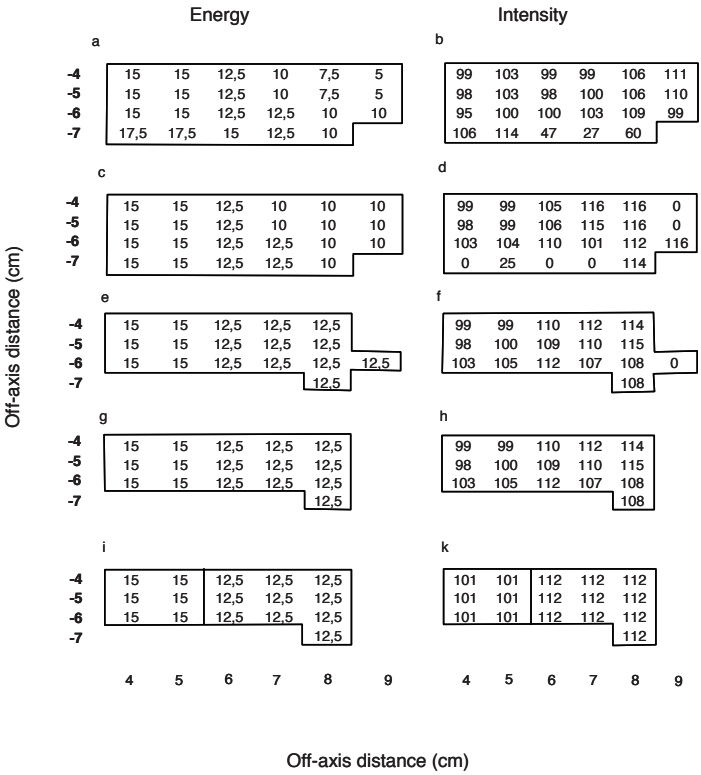

Figure 10. Example of the manual iterative process from the energy-matrix reduced plan to the segmented. The location of the segment shown in this figure corresponds to the lower right corners of the matrices in Fig. 5 and is described by the off-axis positions. (a) and (b) show the original energy (intensity-weighted mean energy) and the optimiser-assigned intensity as they appear in the energy-matrix reduced plan. (c) and (d) illustrate the replacing of energy "islands" by the adjacent energy and the result of the subsequent intensity optimisation. In the next step (e) the energy is set one step higher if the intensity of >4 beamlets is >115, or to 0 if the intensity is <50. The new generated energy "islands" were again replaced by the adjacent energy. (f) shows the new intensities assigned by the optimiser. (g) and (h) show the next iteration and (i) and (k) the final energy and intensity segments.

The results show that both IMET plans and manual plan deliver a similar dose to the PTV and both IMET plans deliver less dose to heart, lung and surrounding normal tissues, compared with the conventional plan. However, wide-margin compensation decreases dose in heart more than energy compensation dose, but with more dose in surrounding normal tissues (Table 2, see Fig. 4 in Paper III). After the procedures of matrix reduction and segmentation, a deliverable treatment plan with energy- and intensity-segmentation was obtained. The energy matrix contained 8 different energies, each with 2-3 intensity levels. This resulted in 23 segments to be delivered

(Fig. 11). There is no much change in dose distribution in wide-margin compensation plans before, during and after segmentation processes (Table 2, see Fig. 4 in Paper III).

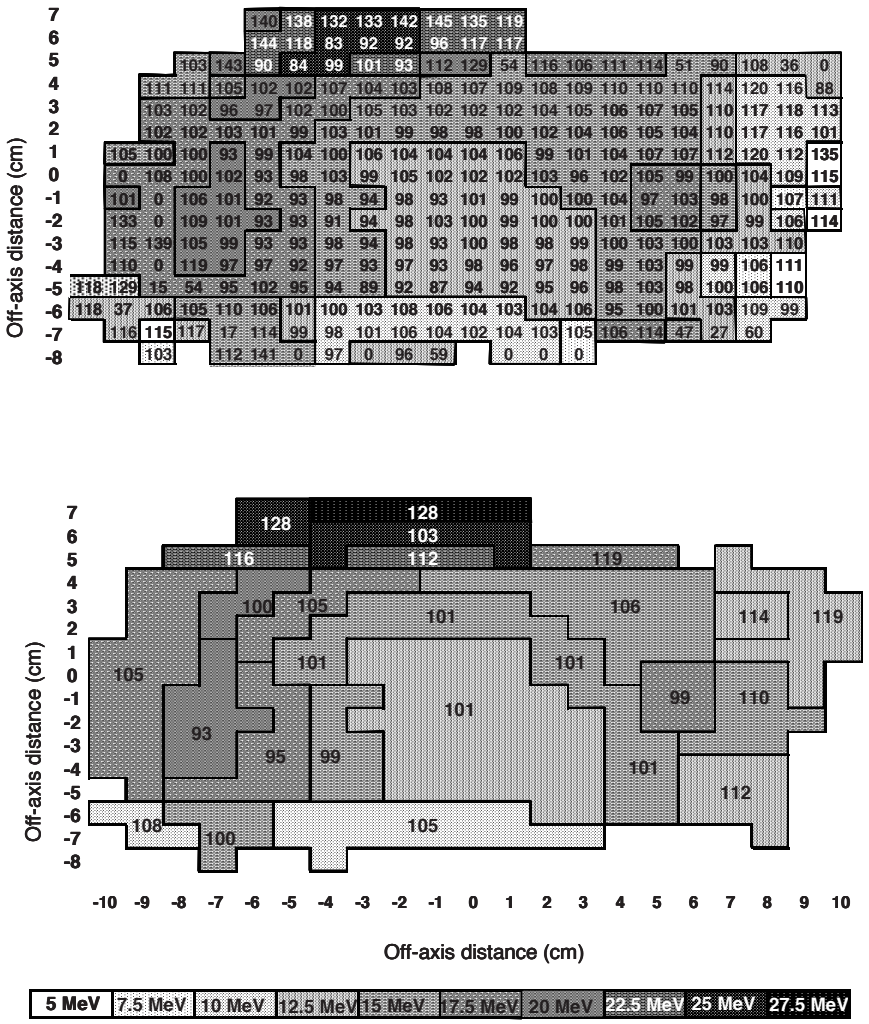

Figure 11. The energy and intensity maps of the energy-matrix reduced plan (a) and the final segmented plan (b). Numbers denote the relative intensities and the different patterns denote different energies.

Table 2. Dose to the PTV, OARs and surrounding tissues.

Type of treatment plan	PTV				Lung		Heart	Surrounding tissues
	D_{min} (Gy)	D_{max} (Gy)	D_{mean} (Gy)	CV (%)	D_{mean} (Gy)	V_{20Gy} (%)	V_{25Gy} (cm^3)	V_{25Gy} (cm^3)
Forward plan	44.5	56.1	50.0	4.6	24.3	54	92 (34%)	1010
Energy compensation	42.8	53.7	50.0	4.3	19.4	43	48 (18%)	490
Wide-margin compensation	44.1	56.5	50.0	4.2	18.1	41	34 (12%)	700
Energy matrix reduced plan	44.1	54.5	50.0	4.6	18.3	42	29 (11%)	660
Segmented plan	44.3	55.2	50.0	5.0	18.6	42	28 (10%)	660

D_{min} and D_{max} are defined as the minimum isodose that encompasses 99 % of the PTV and the maximum isodose that encompasses 1 % of the PTV respectively. D_{mean} is the mean dose. CV is the coefficient of variation. V_{25Gy} is the volume receiving ≥ 25 Gy. Heart volume = 275 cm^3. V_{20Gy} is the percentage of the lung volume receiving more than 20 Gy. “Surrounding tissues” are all tissues outside the PTV and the defined OARs. Energy matrix reduced plan is the intermediate step of manual segmentation.

Side-effects in paediatric therapy and further improvement of the dose conformity with protons (IV)

During the last few decades, the technical improvements in photon therapy have decreased the probability of normal tissue complication (NTCP) without comprising the probabilities of tumour control (TCP). IMXT delivers a high radiation dose to the target volume, but a low dose is absorbed in a large volume of surrounding normal tissues. Some studies have shown that late complications (deterministic effects) also appear after low dose radiation if the follow up time is long enough (27). Particularly in paediatric cancer patient, the stochastic effects, such as radiation induced SLC, have become a major concern after radiotherapy (4). Proton beams may further decrease the integral dose in normal tissue because the physical properties of protons (Fig. 1).

In Paper IV, we carried out a treatment planning comparison study; aim to estimate the risk for late side-effects, particularly radiation induced cancer associated with the technique used. The radiotherapy techniques compared were conventional photon therapy, IMXT, conventional electrons, IMET, and intensity/energy modulated protons (IMPT). CT images of 5 children who diagnosed as 'standard risk' medulloblastoma were selected for this study, since a big number of OARs involved in radiation fields; the patient group is comprised with 2 girls and 3 boys between 6 and 11 years, the median age was 8 years, since the young patient group is of the interest in concerning of radiation induced late complication and SLC.

The total prescribed dose was 23.4 Gy in 13 daily fractions of 1.8 Gy to the PTV as of the present Société International d'Oncologie Pediatrique (SIOP) PNET4 study (54). The prescribed dose for IMPT treatment was converted to the biological equivalent dose (23.4 EGy) by applying a RBE (relative biological effectiveness) factor of 1.1 for protons (55).

The NTCP was estimated for a number of OARs and biological endpoints of interest. The NTCP models used in this study were the relative seriality model (RS model) (56) and the Lyman-Kutcher-Burman model (57-59) (LKB model). The calculation was

performed in BioPlan program (60). The probabilities of acute side-effects, such as radiation pneumonitis (61) and radiation hepatitis (62); the late side-effects, such as radiation induced ischemic heart disease (63), esophagus stricture (64), and small and large bowel obstruction (the volume of abdominal cavity was used for calculation) (59) were estimated respectively. The DVHs were converted to 2 Gy/fraction regimes by using of the linear quadratic model (65), since the parameters of NTCP models were derived with the assumption that the fraction dose is 2 Gy. The α/β values used for DVH conversion were taken from (66).

The risk for secondary lethal cancer (SLC) was estimated according to the model recommended in ICRP recommendations (1), The probability of SLC is the product of the effective dose (E) and the nominal probability coefficient of SLC, and E can be expressed by

$$E = \sum_{T} W_T \cdot \sum_{R} W_R \cdot D_{TR} \qquad \text{(Eq. 6)}$$

where, D_{TR} denotes the mean absorbed dose in a tissue or organ T due to incident radiation R, and W_R and W_T are the radiation modality and tissue weighting factors.

The dose to the red marrow and bone surfaces were not included in the calculation of the effective dose, thus only the risk for lethal solid cancers was considered. The probability for solid SLC has been estimated by the ICRP to 0.045 per Sv for the whole population and adjusted to children by multiplying a factor of 2.5 (1).

Based on the assumption of a linear dose response relationship up to 4 Gy and of a dose-independent relationship for dose above 4 Gy (67), a corrected mean dose to each outlined structures was calculated from DVH data. This means that all doses of > 4Gy in the DVH were given the value of 4 Gy. In order to use this data for a model relating to radiation protection a dose-rate effectiveness factor of 2 has been used (1). This factor has been retained and considered as relevant also for the present purpose (67). A value of 1 for W_R was used for photon and electron beams, and 2 for proton beams (55). The W_T factors recommended in ICRP 60 (1) were used (Table 3). The factors of bone (red marrow and bone surface) and gonads were not included, thus, the sum of

the weighing factors was equal to 0.67 (it would be 1, if whole body was considered). Therefore, the sum of the weighted effective dose of considered organs was renormalized (divided by 0.67). The interleaf leakage and scattering dosage of IMXT was not included in the estimate.

Table 3. Absorbed dose in the volumes of interest.

	Photon Gy (s.d.)	IMXT Gy (s.d.)	Electron Gy (s.d.)	IMET Gy (s.d.)	IMPT Gy (s.d.)
Target					
PTV					
Minimum dose	20.4 (0.5)	19.8 (1.5)	19.5 (0.4)	18.1 (0.6)	19.0 (0.9)
Maximum dose	26.0 (0.2)	26.8 (1.3)	25.6 (0.5)	27.4 (0.8)	27.2 (1.5)
Mean dose	23.4 (0.0)	23.2 (0.2)	23.4 (0.0)	23.3 (0.0)	23.5 (0.4)
Vertebral bodies					
Minimum dose	17.6 (0.8)	15.1 (1.3)	12.9 (4.0)	12.7 (0.6)	11.7 (0.9)
Maximum dose	24.8 (0.5)	26.4 (1.6)	25.5 (0.5)	24.8 (0.3)	25.9 (0.1)
Mean dose	19.5 (1.4)	20.7 (0.6)	19.9 (1.1)	20.1 (0.4)	22.1 (0.1)
OARs (Mean doses)					
Thyroid gland	8.2 (6.3)	4.7 (0.5)	6.3 (3.1)	3.8 (0.3)	0.0 (0.0)
Breast	0.3 (0.2)	0.9 (0.2)	0.2 (0.1)	0.3 (0.0)	0.0 (0.0)
Heart	11.9 (0.9)	4.8 (0.3)	6.1 (1.0)	2.2 (0.5)	0.0 (0.0)
Esophagus	18.2 (0.6)	13.2 (0.7)	16.2 (1.1)	9.4 (0.7)	2.3 (0.4)
Lung	3.0 (0.6)	6.5 (0.5)	3.2 (0.6)	2.0 (0.5)	2.2 (0.1)
Liver	5.5 (0.4)	5.6 (0.2)	2.2 (0.3)	1.2 (0.3)	0.0 (0.0)
Pancreas	13.5 (2.7)	9.2 (1.6)	6.0 (1.6)	4.9 (1.7)	0.0 (0.0)
Spleen	0.6 (0.2)	3.8 (0.5)	0.4 (0.3)	0.2 (0.1)	0.0 (0.0)
Stomach	4.1 (1.4)	6.9 (0.8)	3.2 (1.4)	1.8 (0.6)	0.1 (0.1)
Kidney	2.7 (0.5)	8.9 (0.7)	3.3 (0.8)	1.7 (0.4)	1.3 (0.1)
Abdominal cavity	6.7 (0.9)	7.6 (0.9)	4.7 (1.0)	3.3 (0.7)	0.2 (0.1)
Patient outline	4.7 (0.6)	5.3 (0.2)	4.0 (0.8)	2.2 (0.3)	1.2 (0.1)

All five techniques produced a clinically acceptable dose distribution in the primary and secondary targets. The minimum dose to vertebral body is lower with other techniques compare with conventional photon technique, but it might not cause problem with bone growth (68).

The absorbed doses in the OARs varied considerably with the treatment technique used (Table 3). The IMPT resulted in a significantly lower mean dose to the different OARs except for the lungs compared with all the others techniques, and many of the OARs remained unirradiated. The IMXT delivered significant higher mean doses to the breast, lung, spleen, stomach and kidney than the conventional photon and

electron-techniques. As would be expected, conventional photon and electron techniques gave the highest doses in the thyroid gland and esophagus. Lower mean doses were observed in most OARs with IMET than with the IMXT, photon and electron beam techniques.

Applying the different NTCP models resulted in calculated probabilities for acute and late side-effects that were close to zero for different OARs and all techniques.

Table 4 shows the mean doses after correction (D_{TR}) in OARs and the corresponding risks for SLC. There is a large variation of the estimated risk depending on the technique used. The highest risk estimated for SLC was equal to, 30 %, after IMXT, while the lowest was 4 %, after IMPT were estimated for SLC. For the proton technique we also estimated the potential contributions from secondary neutrons by using measurements and Monte-Carlo simulations performed by Schneider U., et al. for the PSI treatment facility (69). They observed an additional dose burden to ORAs due to secondary neutrons ranging from 0.002 Sv to 0.004 Sv per treatment Gy. Based on these numbers a conservative estimate of the effective neutron dose accumulated in all OARs lead to an additional dose burden of 0.002 Sv (i.e. the total effective dose was 0.0468 Sv). Then the contribution of neutron to the risk of SLC should be in the order of 1%. The effective dose from IMXT was significantly higher than the other techniques ($p=0.002$ in all patients). IMET resulted in a lower effective dose compared with conventional photons beam, IMXT and conventional electrons beam ($p=0.002$ in all patients). IMPT resulted in the lowest effective dose in all comparisons ($p=0.002$ in all patients). Conventional photon and electron techniques resulted in similar effective doses.

Table 4. Estimates of the risk of secondary lethal cancer (solid cancers)

		Photon		IMXT		Electron		IMET		IMPT	
	W_T	D_{TR} (Gy)	$E_{TR} \times W_T$ (Sv)	D_{TR} (Gy)	$E_{TR} \times W_T$ (Sv)	D_{TR} (Gy)	$E_{TR} \times W_T$ (Sv)	D_{TR} (Gy)	$E_{TR} \times W_T$ (Sv)	D_{TR} (Gy)	ETR × WT [a] (Sv)
Esophagus	0.05	3.95	0.20	4.00	0.20	3.99	0.20	3.99	0.20	1.44	0.13
Thyroid	0.05	2.98	0.15	3.01	0.15	3.58	0.18	3.22	0.16	0.01	0.00
Lung	0.12	1.43	0.17	3.12	0.37	1.77	0.21	1.03	0.12	0.15	0.02
Breast	0.05	1.05	0.05	2.35	0.12	0.68	0.03	0.05	0.00	0.01	0.00
Liver	0.05	2.15	0.11	3.05	0.15	1.73	0.09	0.92	0.05	0.02	0.00
Stomach	0.12	2.03	0.24	3.67	0.44	2.22	0.27	1.27	0.15	0.04	0.01
Abdominal cavity	0.20[b]	1.17	0.23	1.69	0.34	1.23	0.24	0.96	0.19	0.06	0.02
Patient outline	0.03[c]	0.82	0.02	1.11	0.03	1.33	0.02	0.38	0.01	0.15	0.01
Effective Dose [d]			1.761		2.696		1.863		1.326		0.306
Total risk of SLC			**0.198**		**0.303**		**0.210**		**0.149**		**0.034** [e]

W_T: Tissue weighting factors. Gonads, red marrow and bone surface were excluded (40)

E_{TR}: Equivalent dose: effective dose to each organ

[a] : a beam quality factor of 2 was applied to proton technique (41)

[b]: W_T includes the factors for colon, urinary bladder and remaining organs (adrenals, small intestine, kidneys, pancreas spleen and uterus)

[c]: W_T includes the factors for skin and remaining organs (brain, muscle and thymus)

[d]: Sum of weighted doses renormalized with the sum of considered weighting factors

[e] : the total risk of SLC for IMPT is 0.040 when the contribution of neutron is taken account

SLC: secondary lethal cancer

Conclusions

The experiments conducted in this study show that the biological effectiveness of radiotherapy can be influenced significantly by a prolonged fraction time in the order of 10-20 minutes. Such changes in radiotherapy may be introduced by more complex treatment techniques such as IMRT. The effect is underestimated by biological models (Paper I). To reach the same cell kill, either fraction size or number of fractions would need to be increased (15-19% for cells used in this study). However, correction is extremely difficult to make in a safe way. The reason is that tissues with longer $T_{1/2}$, as is the case for many normal tissues, would be less spared by the long fraction times and thus, would be subjected to more severe radiation effects. Since biological models are still of limited value in this situation it should be a goal for new radiotherapy techniques to keep the fraction time as short as possible. The findings in this study have later been supported by other experimental (70) and clinical studies (71).

IMXT can be improved with a mixed electron and photon technique for the treatment of a deep-seated target, such as head and neck cancer (Paper II). This study shows that the mixed electron and photon technique delivers a smaller integral dose to normal tissues than photon IMRT while maintaining a comparable dose distribution in the target. In addition, the DVHs of spinal cord and brainstem indicate that there is a margin for further improvement of the mixed beam plans. It is also noteworthy that the treatment plans of this investigation were produced in two completely different ways. The mixed electron and photon technique was planned by a manual procedure that restricted the number of iterations and thus leading to a less than optimal result. The IMRT plans were made with fully automatic optimisation. It is therefore reasonable to believe that if similar tools were available in both cases the results might well be more advantageous for the mixed electron and photon technique. This might particularly be the case if electron beams could be optimised together with photon IMRT. For that reason we believe that this method should be further investigated using optimizing algorithms for electrons. This will also allow comparative studies based on more cases than with this laborious forward planning technique. The mixed beam technique also has the potential of a shorter fraction delivery time than the pure photon IMRT owing

to the smaller number of segments. Thus, the effects of prolonged fraction time should decrease.

Optimised electron plans will contain both energy and intensity modulation which means that the number of segments will often be too large for being delivered in an effective way in clinical routine. In IMXT there are methods for reducing the number of segments that have to be treated, often by the use of a so called “sequencer”. For making optimised electron beams clinically useful a corresponding procedure as for IMXT could be useful. For this reason, a method has been developed to transform the results from an electron optmiser to a deliverable treatment plan with a three-step procedure (Paper III). All such procedures, including optimisation and segmentation, would be possible to computerise. This method was tested with a clinical case that had a left-sided breast cancer after mastectomy. It resulted in a plan with 8 electron energies and 23 segments which can be delivered in a reasonable time frame without destroying the dose distribution that was primarily achieved with the optimiser.

In Paper IV the most commonly used NTCP models predicted very low risks for side-effects for all five radiation techniques, despite the considerable variation in absorbed dose to the surrounding OARs. This is probably partly due to the low total dose. However, the predictive ability of the NTCP models has actually not been fully tested as yet, especially in the case of late side-effects (e.g. cardiac mortality). Another noteworthy aspect when using NTCP models is that the dose distribution and clinical data on which the models are based reflect irradiation conditions in the specific patient groups. To our knowledge, no available NTCP parameters are based on data sets derived from a paediatric population. Furthermore, the relevant end-points in a paediatric population might not always be the same as in an adult population. In paediatric populations, the risk for secondary radiation induced cancer should be of concern. A model for calculating the risk for SLC has been proposed by ICRP 60 (1). It was not originally intended for radiotherapy, but it is one of the few models available today that can be applied in this situation. In radiation protection, lower doses than those relevant for radiotherapy are usually considered. Therefore, an assumption that the risk of cancer increases linearly with dose below 4 Gy and levels

out at doses above about 4 Gy was made (Paper IV). This hypothesis might make the risk estimates slightly conservative. On the other hand, any effects of cell kill and a consequent decrease in cancer risk at high doses were not taken into consideration due to the lack of available data on which to base such a correction. The estimated risks of radiation induced SLC in treatment of the spinal canal in medulloblastoma differ substantially depending on the techniques used. The estimated risks are 30 % (IMXT), 20% (conventional photons or electrons),15% (IMET) and 4% (IMPT). The absolute risks should probably be regarded with caution due to the uncertainties in the estimates. However, the relative differences between the treatments are probably only slightly influenced by these uncertainties. To minimise the risk of cancer induction, IMPT should be the treatment of choice. If proton therapy is not available, advanced electron therapy may provide a better alternative to conventional photon therapy.

Acknowledgements

The work on this thesis has given me the opportunity to meet and work with a lot of wonderful and interesting people. I would like to thank all persons who very generously shared their experiences for the benefit my project and ultimately, hopefully, for future patients. I would like to especially express my deep and sincere gratitude to the following persons.

Associate professor Björn Zackrisson, my main supervisor and good friend who has helped me with his great scientific expertise to develop my scientific capability, for being an endless source of ideas, inspiration, advices, and encouragement, and for his excellent scientific guidance throughout this work.

Professor Mikael Karlsson, co-supervisor, for his kind scientific guides and discussions and support during this work, and for the friendly and warm relationship he has offered me.

Thomas Björk-Eriksson, co-supervisor, for his expertise, enthusiastic interest in my work and never-failing support.

Lennart Olofsson for constructive collaboration and co-authorship, helping me went through the first phase of my research; Per-Olov Löfroth and Lennart Johansson for constructive collaboration and co-authorship; Karl-Axel Johansson for his advices and being patient with my slow response; Giovanna Gagliardi for her contribution with her radiobiological knowledge.

Uwe Oelfke and Simeon Nill for kindly providing the KonRad program, solving technical problems with the computer and co-authorship.

Anna Wernblom and Carina Ahlgren for efficient secretarial work and a lot of help with many practical problems.

Magnus Karlsson and Mikael Blomquist for interesting discussions and solving technical problems; Rikard Hagström for solving seemingly endless computer problems.

Sun Qiyin, the former director of Zibo Wanjie Hospital. Without his inspiration and help, I would not have had the opportunity to do this work. Sun Qiyu, the Chairman of Zibo Wanjie Group. Without his support, I would never have been able to reach this far.

Finally, I would like to thank my parents, my wife and daughter. They encourage and support me with their love; I was able to complete this thesis.

The work presented here was supported by grants from the Lion's Cancer Research Foundation at Umeå University Hospital and partly from Zibo Wanjie Hospital, Shandong, China.

References

1. Recommendations of the International Commission on Radiological Protection. ICRP Publication 60, Ann ICRP 1990; 21(1–3).
2. UNSCEAR, Sources and effects of ionizing radiation.United Nations Scientific Committee on the Effects of Atomic Radiation 2000 report to the General Assembly, with Annexes. Volume I: Sources. 2000: New Uork, NY: Unite Nations; 2000.
3. Lomax, A. Intensity modulation methods for proton radiotherapy. Phys Med Biol 1999; 44:185-205.
4. Suit, H, S Goldberg, A Niemierko, et al. Proton beams to replace photon beams in radical dose treatments. Acta Oncol 2003; 42:800-8.
5. Purdy, JA. 3-D radiation treatment planning: a new era. Front Radiat Ther Oncol 1996; 29:1-16.
6. Bjarngard, BE. Optimization in radiation therapy. Int J Radiat Oncol Biol Phys 1977; 2:381-2.
7. Chin, LM, PK Kijewski, GK Svensson, and BE Bjarngard. Dose optimization with computer-controlled gantry rotation, collimator motion and dose-rate variation. Int J Radiat Oncol Biol Phys 1983; 9:723-9.
8. Intensity-Modulated-Radiation-Therapy-Collaborative-Working-Group. Intensity-modulated radiotherapy: current status and issues of interest. Int J Radiat Oncol Biol Phys 2001; 51:880-914.
9. Bortfeld, T, AL Boyer, W Schlegel, DL Kahler, and TJ Waldron. Realization and verification of three-dimensional conformal radiotherapy with modulated fields. Int J Radiat Oncol Biol Phys 1994; 30:899-908.
10. Ling, CC, C Burman, CS Chui, et al. Conformal radiation treatment of prostate cancer using inversely-planned intensity-modulated photon beams produced with dynamic multileaf collimation. Int J Radiat Oncol Biol Phys 1996; 35:721-30.
11. Verhey, LJ. Comparison of three-dimensional conformal radiation therapy and intensity-modulated radiation therapy systems. Semin Radiat Oncol 1999; 9:78-98.
12. Tubiana, M and F Eschwege. Conformal radiotherapy and intensity-modulated radiotherapy--clinical data. Acta Oncol 2000; 39:555-67.
13. Gregoire, V and P Maingon. Intensity-modulated radiation therapy in head and neck squamous cell carcinoma: an adaptation of 2-dimensional concepts or a reconsideration of current clinical practice. Semin Radiat Oncol 2004; 14:110-20.
14. Dearnaley, DP, VS Khoo, AR Norman, et al. Comparison of radiation side-effects of conformal and conventional radiotherapy in prostate cancer: a randomised trial. Lancet 1999; 353:267-72.
15. Eisbruch, A, RK Ten Haken, HM Kim, LH Marsh, and JA Ship. Dose, volume, and function relationships in parotid salivary glands following conformal and intensity-modulated irradiation of head and neck cancer. Int J Radiat Oncol Biol Phys 1999; 45:577-87.

16. Koper, PC, JC Stroom, WL van Putten, et al. Acute morbidity reduction using 3DCRT for prostate carcinoma: a randomized study. Int J Radiat Oncol Biol Phys 1999; 43:727-34.

17. Eisbruch, A, LH Marsh, MK Martel, et al. Comprehensive irradiation of head and neck cancer using conformal multisegmental fields: assessment of target coverage and noninvolved tissue sparing. Int J Radiat Oncol Biol Phys 1998; 41:559-68.

18. Chao, KS, FJ Wippold, G Ozyigit, BN Tran, and JF Dempsey. Determination and delineation of nodal target volumes for head-and-neck cancer based on patterns of failure in patients receiving definitive and postoperative IMRT. Int J Radiat Oncol Biol Phys 2002; 53:1174-84.

19. Wu, Q, R Mohan, M Morris, A Lauve, and R Schmidt-Ullrich. Simultaneous integrated boost intensity-modulated radiotherapy for locally advanced head-and-neck squamous cell carcinomas. I: dosimetric results. Int J Radiat Oncol Biol Phys 2003; 56:573-85.

20. Fraass, BA, ML Kessler, DL McShan, et al. Optimization and clinical use of multisegment intensity-modulated radiation therapy for high-dose conformal therapy. Semin Radiat Oncol 1999; 9:60-77.

21. Hong, L, M Hunt, C Chui, et al. Intensity-modulated tangential beam irradiation of the intact breast. Int J Radiat Oncol Biol Phys 1999; 44:1155-64.

22. Lomax, AJ, L Cella, D Weber, JM Kurtz, and R Miralbell. Potential role of intensity-modulated photons and protons in the treatment of the breast and regional nodes. Int J Radiat Oncol Biol Phys 2003; 55:785-92.

23. Huang, E, BS Teh, DR Strother, et al. Intensity-modulated radiation therapy for pediatric medulloblastoma: early report on the reduction of ototoxicity. Int J Radiat Oncol Biol Phys 2002; 52:599-605.

24. Mell, LK, JC Roeske, and AJ Mundt. A survey of intensity-modulated radiation therapy use in the United States. Cancer 2003; 98:204-11.

25. Zhen, W, RB Thompson, and CA Enke. Intensity-modulated radiation therapy (IMRT): the radiation oncologist's perspective. Med Dosim 2002; 27:155-9.

26. Galvin, JM, G Ezzell, A Eisbrauch, et al. Implementing IMRT in clinical practice: a joint document of the American Society for Therapeutic Radiology and Oncology and the American Association of Physicists in Medicine. Int J Radiat Oncol Biol Phys 2004; 58:1616-34.

27. Rubin, P, CJ Johnston, JP Williams, S McDonald, and JN Finkelstein. A perpetual cascade of cytokines postirradiation leads to pulmonary fibrosis. Int J Radiat Oncol Biol Phys 1995; 33:99-109.

28. Joiner, MC, B Marples, P Lambin, SC Short, and I Turesson. Low-dose hypersensitivity: current status and possible mechanisms. Int J Radiat Oncol Biol Phys 2001; 49:379-89.

29. Chang, SX, TJ Cullip, and KM Deschesne. Intensity modulation delivery techniques: "step & shoot" MLC auto-sequence versus the use of a modulator. Med Phys 2000; 27:948-59.

30. Verhey, LJ. Physical considerations in the use of intensity modulated radiotherapy to produce three-dimensional conformal dose distributions. J Jpn Soc Ther Radiol Oncol 2000; 12:191-203.

31. Turesson, I, G Notter, I Wickstrom, KA Johansson, and S Eklund. The influence of irradiation time per treatment session on acute and late skin reactions: a study on human skin. Radiother Oncol 1984; 2:235-45.

32. Barendsen, GW. Dose fractionation, dose rate and iso-effect relationships for normal tissue responses. Int J Radiat Oncol Biol Phys 1982; 8:1981-97.

33. Lea, DE and DG Catheside. The mechanism of induction by radiation of chromosome aberrations in tradescantia. J Genet 1942; 44:216-54.

34. Dale, RG. The application of the linear-quadratic dose-effect equation to fractionated and protracted radiotherapy. Br J Radiol 1985; 58:515-28.

35. Thames, HD. An 'incomplete-repair' model for survival after fractionated and continuous irradiations. Int J Radiat Biol Relat Stud Phys Chem Med 1985; 47:319-39.

36. Karlsson, M and B Zackrisson. Exploration of new treatment modalities offered by high energy (up to 50 MeV) electrons and photons. Radiother Oncol 1997; 43:303-9.

37. Korevaar, EW, RJ van Vliet, E Woudstra, BJ Heijmen, and H Huizenga. Sharpening the penumbra of high energy electron beams with low weight narrow photon beams. Radiother Oncol 1998; 48:213-20.

38. Korevaar, EW, BJ Heijmen, E Woudstra, H Huizenga, and A Brahme. Mixing intensity modulated electron and photon beams: combining a steep dose fall-off at depth with sharp and depth-independent penumbras and flat beam profiles. Phys Med Biol 1999; 44:2171-81.

39. Karlsson, M and B Zackrisson. Matching of electron and photon beams with a multi-leaf collimator. Radiother Oncol 1993; 29:317-26.

40. Zackrisson, B and M Karlsson. Matching of electron beams for conformal therapy of target volumes at moderate depths. Radiother Oncol 1996; 39:261-70.

41. Klein, EE. Modulated electron beams using multi-segmented multileaf collimation. Radiother Oncol 1998; 48:307-11.

42. Olofsson, L, X Mu, S Nill, et al. Intensity modulated radiation therapy with electrons using algorithm based energy/range selection methods. Radiother Oncol 2004; 73:223-31.

43. Perkins, GH, MD McNeese, JA Antolak, et al. A custom three-dimensional electron bolus technique for optimization of postmastectomy irradiation. Int J Radiat Oncol Biol Phys 2001; 51:1142-51.

44. Asell, M, S Hyodynmaa, A Gustafsson, and A Brahme. Optimization of 3D conformal electron beam therapy in inhomogeneous media by concomitant fluence and energy modulation. Phys Med Biol 1997; 42:2083-100.

45. Ma, CM, M Ding, JS Li, et al. A comparative dosimetric study on tangential photon beams, intensity-modulated radiation therapy (IMRT) and modulated electron radiotherapy (MERT) for breast cancer treatment. Phys Med Biol 2003; 48:909-24.

46. Wu, Q, M Manning, R Schmidt-Ullrich, and R Mohan. The potential for sparing of parotids and escalation of biologically effective dose with intensity-modulated

radiation treatments of head and neck cancers: a treatment design study. Int J Radiat Oncol Biol Phys 2000; 46:195-205.

47. Lin, A, HM Kim, JE Terrell, et al. Quality of life after parotid-sparing IMRT for head-and-neck cancer: a prospective longitudinal study. Int J Radiat Oncol Biol Phys 2003; 57:61-70.

48. Cozzi, L, A Fogliata, A Bolsi, G Nicolini, and J Bernier. Three-dimensional conformal vs. intensity-modulated radiotherapy in head-and-neck cancer patients: comparative analysis of dosimetric and technical parameters. Int J Radiat Oncol Biol Phys 2004; 58:617-24.

49. Glatstein, E. Intensity-modulated radiation therapy: the inverse, the converse, and the perverse. Semin Radiat Oncol 2002; 12:272-81.

50. Klein, EE, Z Li, and DA Low. Feasibility study of multileaf collimated electrons with a scattering foil based accelerator. Radiother Oncol 1996; 41:189-96.

51. Moran, JM, MK Martel, IA Bruinvis, and BA Fraass. Characteristics of scattered electron beams shaped with a multileaf collimator. Med Phys 1997; 24:1491-8.

52. Karlsson, MG, M Karlsson, and CM Ma. Treatment head design for multileaf collimated high-energy electrons. Med Phys 1999; 26:2161-7.

53. Blomquist, M, MG Karlsson, B Zackrisson, and M Karlsson. Multileaf collimation of electrons--clinical effects on electron energy modulation and mixed beam therapy depending on treatment head design. Phys Med Biol 2002; 47:1013-24.

54. Coles, CE, AC Hoole, SV Harden, et al. Quantitative assessment of inter-clinician variability of target volume delineation for medulloblastoma: quality assurance for the SIOP PNET 4 trial protocol. Radiother Oncol 2003; 69:189-94.

55. Recommendations of the International Commission on Radiological Protection. ICRP Publication 92, . Ann ICRP 2003; 33(4).

56. Kallman, P, A Agren, and A Brahme. Tumour and normal tissue responses to fractionated non-uniform dose delivery. Int J Radiat Biol 1992; 62:249-62.

57. Lyman, JT. Complication probability as assessed from dose-volume histograms. Radiat Res Suppl 1985; 8:S13-9.

58. Kutcher, GJ and C Burman. Calculation of complication probability factors for non-uniform normal tissue irradiation: the effective volume method. Int J Radiat Oncol Biol Phys 1989; 16:1623-30.

59. Burman, C, GJ Kutcher, B Emami, and M Goitein. Fitting of normal tissue tolerance data to an analytic function. Int J Radiat Oncol Biol Phys 1991; 21:123-35.

60. Sanchez-Nieto, B and AE Nahum. BIOPLAN: software for the biological evaluation of. Radiotherapy treatment plans. Med Dosim 2000; 25:71-6.

61. Gagliardi, G, I Lax, S Soderstrom, G Gyenes, and LE Rutqvist. Prediction of excess risk of long-term cardiac mortality after radiotherapy of stage I breast cancer. Radiother Oncol 1998; 46:63-71.

62. Dawson, LA, D Normolle, JM Balter, et al. Analysis of radiation-induced liver disease using the Lyman NTCP model. Int J Radiat Oncol Biol Phys 2002; 53:810-21.

63. Gagliardi, G, I Lax, A Ottolenghi, and LE Rutqvist. Long-term cardiac mortality after radiotherapy of breast cancer--application of the relative seriality model. Br J Radiol 1996; 69:839-46.

64. Mavroidis, P, G Laurell, T Kraepelien, et al. Determination and clinical verification of dose-response parameters for esophageal stricture from head and neck radiotherapy. Acta Oncol 2003; 42:865-81.

65. Wheldon, TE, C Deehan, EG Wheldon, and A Barrett. The linear-quadratic transformation of dose-volume histograms in fractionated radiotherapy. Radiother Oncol 1998; 46:285-95.

66. Steel. G. Gordon, Basic clinical radiobiology. 3. ed. ed. 2002, London: Arnold.

67. Hall, EJ and CS Wuu. Radiation-induced second cancers: the impact of 3D-CRT and IMRT. Int J Radiat Oncol Biol Phys 2003; 56:83-8.

68. Bloom, HJ, EN Wallace, and JM Henk. The treatment and prognosis of medulloblastoma in children. A study of 82 verified cases. Am J Roentgenol Radium Ther Nucl Med 1969; 105:43-62.

69. Schneider, U, S Agosteo, E Pedroni, and J Besserer. Secondary neutron dose during proton therapy using spot scanning. Int J Radiat Oncol Biol Phys 2002; 53:244-51.

70. Shibamoto, Y, M Ito, C Sugie, H Ogino, and M Hara. Recovery from sublethal damage during intermittent exposures in cultured tumor cells: implications for dose modification in radiosurgery and IMRT. Int J Radiat Oncol Biol Phys 2004; 59:1484-90.

71. Wang, JZ, XA Li, WD D'Souza, and RD Stewart. Impact of prolonged fraction delivery times on tumor control: a note of caution for intensity-modulated radiation therapy (IMRT). Int J Radiat Oncol Biol Phys 2003; 57:543-52.